

Compounds of Silicon and Homologues, 134^[+] Supersilyl Compounds of Boron and Homologues, 10^[+]

Tri(supersilyl)dialanyl (*t*Bu₃Si)₃Al₂[•] and Tetra(supersilyl)cyclotrialanyl (*t*Bu₃Si)₄Al₃[•] – New Stable Radicals of a Group 13 Element from Thermolysis of (*t*Bu₃Si)₄Al₂

Nils Wiberg,^{*,[a]} Thomas Blank,^[a] Wolfgang Kaim,^[b] Brigitte Schwederski,^[b] and Gerald Linti^[c]

Keywords: Ab initio calculations / Aluminum / ESR Spectroscopy / Radicals / Silicon

The thermolysis of tetra(supersilyl)dialane R^{*}₂Al–AlR^{*}₂ (R^{*} = Si*t*Bu₃ = Supersilyl) in heptane or cyclohexane at 50 °C leads under Al–Al dissociation reversibly to monoalanyl radicals [R^{*}₂Al][•], which could be trapped by hydrogen or iodine (formation of R^{*}₂AlH, R^{*}₂AlI). Simultaneously, SiAl dissociation and elimination of supersilyl radicals *t*Bu₃Si[•] leads irreversibly and slowly to radicals [R^{*}₂Al–AlR^{*}][•], the existence of which could be established by ESR spectroscopy. The structure was clarified by ab initio calculations (nearly planar Si₂Al–AlSi and linear Al–Al–Si skeleton; short Al–Al dis-

tance). By thermolyzing R^{*}₂Al–AlR^{*}₂ at 100 °C, the radical [R^{*}₄Al₃][•] (ESR spectroscopically detected) and the *tetrahedro*-tetraalane R^{*}₄Al₄ (NMR spectroscopically seen) are formed via radicals [R^{*}₃Al₂][•]; the supersilyl radicals *t*Bu₃Si[•], formed at the same time, are stabilized by dimerization to superdisilane R^{*}–R^{*} and by taking up hydrogen, giving supersilane R^{*}–H. According to X-ray structure analysis, the Al atoms in [R^{*}₄Al₃][•] are located at the corners of a triangle; one Al atom is connected with two groups R^{*}, the remaining two Al atoms each bind one substituent R^{*} in different ways.

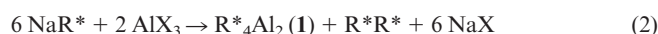
Introduction

Unlike aluminum triorganyls R₃Al with aluminum in the oxidation state III, which were synthesized for the first time in the middle of the 19th century,^[1] aluminum organyls R_{*m*}Al_{*n*} with aluminum in the oxidation state < III were unknown for a long time because of their high tendency for disproportionation into R₃Al and Al.^[2,3] Therefore, dehalogenations of diorganylaluminum chlorides R₂AlCl with substituents R of *lower to medium bulkiness* like CH₂R' (R' = H, Me, Et, CMe₃, SiMe₃) or 2,4,6-Me₃C₆H₂ lead to R₃Al and Al. The results were interpreted as disproportionations of intermediately formed tetraorganylalanes R₄Al₂.^[2] According to Equation (1), the latter disproportionations may proceed via aluminum cluster compounds R_{*m*}Al_{*n*}, which are formed from starting materials with a higher *m/n* ratio and transform into products with a lower *m/n* ratio.



The substituents R in R₂AlCl with *higher bulkiness* like CH(SiMe₃)₂ or 2,4,6-*i*Pr₃C₆H₂ inhibit this disproportionation. As a result of this, the dehalogenation of R₂AlCl stopped under normal conditions at the tetraorganylalanes R₄Al₂ with aluminum in the oxidation state II.^[2] Exactly the same holds for the bulky substituent Supersilyl (R^{*} = Si*t*Bu₃), which also allows the isolation of a dialane(4), namely tetra(supersilyl)dialane R^{*}₄Al₂ (**1**), at room temperature.^[4] At higher temperatures, compound **1**, amongst others, decomposes into the *tetrahedro*-tetraalane R^{*}₄Al₄ with aluminum in the oxidation state I (and the *m/n* ratio decreases from 2 to 1).^[4]

In this paper, two established intermediates of the mentioned dialane(4) thermolysis will be introduced, namely the dialanyl radical R^{*}₃Al₂[•] (**2**) and the cyclotrialanyl radical R^{*}₄Al₃[•] (**3**). The starting material R^{*}₄Al₂ (**1**) required for the thermolysis is – as was recently reported – easily prepared in quantitative yields by reaction of supersilyl sodium NaR^{*} with aluminum trihalides AlX₃ (X = Cl, Br) in heptane at room temperature according to Equation (2):



Isolable reaction intermediates in the formation of the red **1** are yellow di(supersilyl)aluminum halides R^{*}₂AlX (AlX₃ + 2 NaR^{*} → R^{*}₂AlX + 2 NaX).^[5] Excess supersilyl-sodium converts R^{*}₂AlX into the radicals R^{*}₂Al[•] and R^{*}[•], which, for steric reasons, cannot combine to form R₃Al, but

[⁺] Part 133: N. Wiberg, A. Wörner, D. Fenske, H. Nöth, J. Knizek, K. Polborn, *Angew. Chem.* **2000**, *112*, 1908–1912; *Angew. Chem. Int. Ed.* **2000**, *39*, 1838–1842.

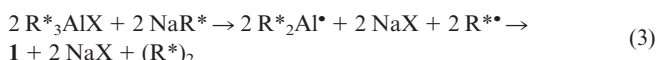
[⁺,⁺] Part 9: N. Wiberg, T. Blank, A. Purath, H. Schnöckel, *Angew. Chem.* **1999**, *111*, 2745–2748; *Angew. Chem. Int. Ed.* **1999**, *38*, 2563–2565.

[^a] Department Chemie der Universität München, Butenandtstraße 5–13 (Haus D), D-81377 München, Germany

[^b] Institut für Anorganische Chemie der Universität Stuttgart, Pfaffenwaldring 55, D-70550 Stuttgart, Germany

[^c] Institut für Anorganische Chemie der Universität Karlsruhe, Engesserstraße, Geb. 30.45, D-76128 Karlsruhe, Germany

instead dimerize to $R^*_2Al-AlR^*_2$ and R^*R^* according to Equation (3) (see also Scheme 1):



Formation of Dialanyl Radicals $R^*_4Al_3^*$ and Cyclotrialanyl Radicals $R^*_4Al_3^*$

The first step of thermolysis of **1** may involve a homolytic dissociation of the Si–Al or the Al–Al bonds (cf. Scheme 1). Mild warming of **1** in heptane or cyclohexane to 50 °C leads by fast and reversible Al–Al bond dissociation to the di(supersilyl)alanyl radical $R^*_2Al^*$ in low equilibrium concentration. This is supported – as we mentioned previously^[4] – by the reaction of **1** with hydrogen or iodine which leads to di(supersilyl)alane R^*_2AlH or di(supersilyl)aluminum iodide R^*_2AlI (cf. Scheme 1). In the absence of trapping reagents for $R^*_2Al^*$ and by heating the solution to 80 °C, compound **1** slowly but irreversibly gives the tri(supersilyl)dialanyl radicals $R^*_3Al_2^*$ (**2**) by Si–Al bond dissociation. The latter transforms slowly and irreversibly into the tetra(supersilyl)cyclotrialanyl radical $R^*_4Al_3^*$ (**3**) and tetra(supersilyl)-*tetrahedro*-tetraalane $R^*_4Al_4$ (**4**) (Scheme 1). Thereby, compound **3** may be formed by reaction of **2** with $R^*_2Al^*$, and compound **4** by reaction of **2** with itself. The simultaneously obtained supersilyl radicals R^*R^* dimerize to superdisilane R^*-R^* (cf. Scheme 1). After heating **1** in heptane or cyclohexane for 4 hours at 70 °C, the dialane(**4**) is completely decomposed and the black-green solution then contains **2**, **3** and **4**, as well as $(R^*)_2$.

By heating the solution to 100 °C, or by heating compound **1** for 10 hours in heptane at 100 °C (reflux), the intermediately formed **2** transforms completely into **3** and

red-violet **4** (cf. Scheme 1; $R^*_4Al_4$ has been prepared previously by a different method and is well characterized).^[6] At the same time the superdisilane $(R^*)_2$ present in the mixture decomposes slowly into supersilyl radicals, which are then stabilized by abstracting H atoms from the chemical surroundings (formation of supersilane R^*-H ; cf. Scheme 1). Compound **3** crystallized after two months from a heptane solution as black-green, paramagnetic, moisture- and air-sensitive crystals. Heating **3** in heptane at higher temperatures transforms the radicals into other products, the identities of which are currently being investigated.

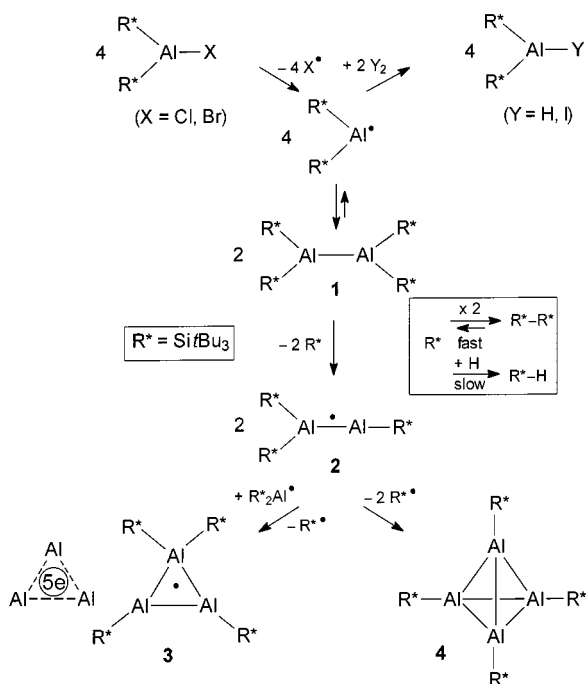
It should be mentioned here that the heavier homologue of **2**, tri(supersilyl)digallanyl $R^*_3Ga_2^*$ forms so easily that the initial stage, tetra(supersilyl)digallane $R^*_4Ga_2$, is not isolable.^[7] Thermolysis of $R^*_3Ga_2^*$ in heptane at 100 °C leads exclusively to tetra(supersilyl)-*tetrahedro*-tetragallane $R^*_4Ga_4$.^[8] This fact supports our proposal in Scheme 1 that the tetrahedranes $R^*_4E_4$ ($E = Al, Ga$) are formed by reaction of $R^*_3E_2^*$ with $R^*_3E_2^*$, and the cyclic radicals $R^*_4E_3^*$ by reaction of $R^*_3E_2^*$ with $R^*_2E^*$ (not present in the case of $R^*_3Ga_2^*$); in fact, $R^*_4Ga_3^*$ has been prepared by another route). However, other mechanisms are also imaginable. Interestingly, dilute solutions of **1** form the *tetrahedro*-tetrahedrane **4** under the action of light.

Unlike $R^*_4Al_2$ and $R^*_3Ga_2^*$, tetra(supersilyl)diindane $R^*_4In_2$ thermolyzes in heptane at 100 °C within 18 hours to octa(supersilyl)dodecaindane $R^*_8In_{12}$.^[9] The diindanyl $R^*_3In_2^*$ and cyclotriindanyl $R^*_4In_3^*$ radicals, which may be reaction intermediates, have not yet been observed by ESR spectroscopy [tetra(supersilyl)-*tetrahedro*-tetraindane $R^*_4In_4$ is not formed under these conditions].

Structure and ESR Spectrum of Dialanyl Radicals $R^*_3Al_2^*$ (**2**)

As mentioned above, the thermolysis of **1** in heptane leads to compounds **2**, **3** and **4**. Until now, only compound **3** has been isolated as crystals from such solutions.

According to ab initio calculations at the RI-DFT level, the structure of the radical **2** is comparable to the structure of the black-blue radical $R^*_3Ga_2^*$, which has previously been examined by an X-ray structure analysis.^[7] Figure 1 shows the results of these calculations^[10] together with selected bond lengths for $R^*_3Al_2^*$ (ab initio calculation) and $R^*_3Ga_2^*$ (X-ray structure analysis). Both radicals show almost a planar Si_2E-ESi skeleton (sum of angles at $E1 = Al1/Ga1$ 359.7/359.3°); in addition, the $E-E-Si$ skeleton is nearly linear (angles at $E2 = Al2/Ga2$ 174.9/170.0; the $E1-E2-Si3$ plane is nearly orthogonal to the $Si1-E1-Si2$ plane). In both cases the $E-E$ distance is comparatively short. This points to an $E-E$ bonding order greater than one. The observed shortening of the $E-E$ bond length in the order $R^*_3Al_2^* \rightarrow R^*_3Ga_2^*$ (2.537 \rightarrow 2.423 Å; difference 0.114 Å) may be due to a reduction of the radius or of the charge separation in the order $Al \rightarrow Ga$ [analogously, the $E-E$ single bond length decreases in the order $Disyl_4Al_2 \rightarrow Disyl_4Ga_2$: 2.660 \rightarrow 2.541 Å; difference 0.119 Å;^[2] $Disyl = CH(SiMe_3)_2$]. According to this, $R^*_3E_2^*$ contains sp^2 - and



Scheme 1. Thermolysis of tetra(supersilyl)dialane **1**

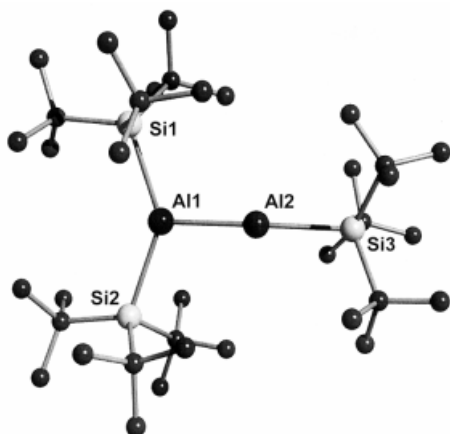
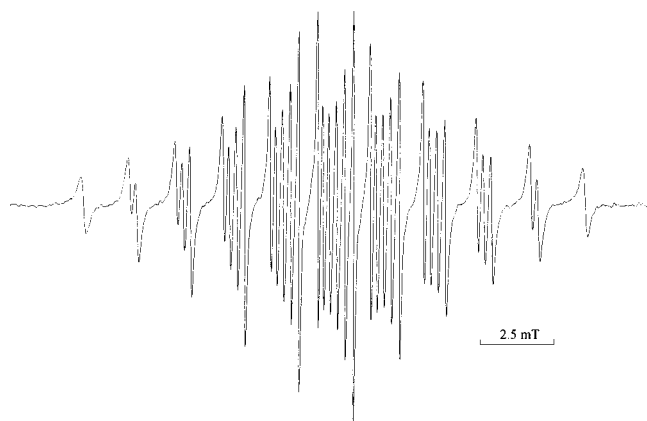


Figure 1. Structure of $R^*_3Al_2\bullet$ (**2**) from RI-DFT calculations; selected calculated bond lengths [Å] and angles [°] (in brackets, for comparison, analogous bond lengths and angles for $R^*_3Ga_2\bullet$; in the latter case, the mean values of two independent molecules in the cell): Al1–Al2 2.537 (2.423), Al1–Si1 2.583 (2.513), Al1–Si2 2.571 (2.499), Al2–Si3 2.562 (2.504); Al2–Al1–Si1 107.87 (109.32), Al2–Al1–Si2 109.58 (109.90), Si1–Al1–Si2 142.21 (140.44), Al1–Al2–Si3 174.90 (170.03)

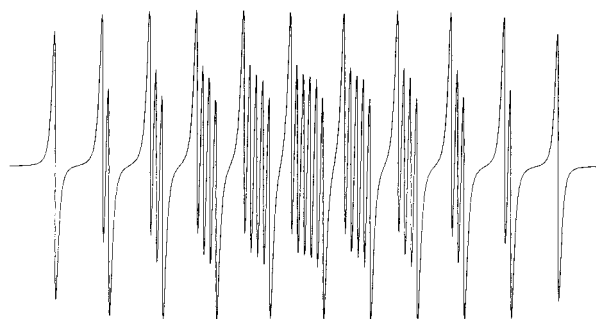
sp-hybridized E atoms, which are connected via two-electron σ - and one-electron π -bonds.

The constitution of **2** is deduced from the ESR spectrum of solutions in pentane or cyclohexane. Well-resolved spectra of **2** are only obtained from alkane solutions of the dialane **1**, which always contain traces of the radical **2**, but no traces of the radical **3**.

Solutions of $R^*_2Al-AlR^*_2$ in alkanes exhibit a simple room-temperature ESR spectrum for the paramagnetic species $[R^*_2Al-AlR^*_2]\bullet$. The hyperfine coupling of the unpaired electron with the two- and the three-coordinate aluminum atom (^{27}Al , nuclear spin $I = 5/2$, 100% nat. abundance) is rather similar and leads to groups of peaks with from one to six EPR lines (Figure 2a). The observed coupling constants are $a(Al1) = 2.18$ mT and $a(Al2) = 1.89$ mT; the isotropic g factor is 2.0011 (cf. Figure 1 for atom numbering and Figure 2b for simulation of the ESR spectrum). As described for a number of related radicals,^[7,11,12] $[R^*_2Al-AlR^*_2]\bullet$ shows a strong anisotropic broadening of the outer lines (Figure 2a). The reason for this known effect is the comparatively slow rotation of the heavy molecule in solution as a result of the large moment of inertia. Therefore, strong anisotropic contributions of the g factor and hyperfine tensors, which result from the π character of the radical electron, are not completely averaged out at room temperature. The strikingly small difference between the two ^{27}Al coupling constants does not allow a clear assignment. Obviously, the π character of the unpaired electron at the center of the two-coordinate Al atom leads to a comparatively low $a(^{27}Al)$ value, whereas the center of the three-coordinate approximately non-radical Al atom has a rather high coupling constant. The latter follows from spin polarization and from the bulkiness of the supersilyl group which may favor a large spin density. The stronger participation of s contributions is illustrated by the generally higher coupling constants for $[R^*_2Al-AlR^*_2]\bullet$ compared to those of



(a)



(b)

Figure 2. ESR spectrum of **2** in *n*-pentane: (a) with strong anisotropic broadening of lines, and (b) its simulation with hyperfine coupling constants $a(Al1) = 2.18$ mT and $a(Al2) = 1.89$ mT

$[R^*_2Al-AlR^*_2]\bullet$ [$R' = CH(SiMe_3)_2$; $a(^{27}Al) = 1.11$ mT]. As the g factor differs only slightly from g (electron) = 2.0023, the radical $[R^*_2Al-AlR^*_2]\bullet$ must be a π -radical. The deviation to lower g agrees with observations for the radical $[R^*_2Ga-GaR^*]\bullet$, which shows clearer effects as a consequence of the higher spin-orbit coupling factor for gallium.^[7]

Structure and ESR Spectrum of the Cyclotrialanyl Radical $R^*_4Al_3\bullet$ (**3**)

The structure of the radicals $R^*_4Al_3\bullet$ (**3**) in the black-green crystals (monoclinic; obtained from heptane) is shown in Figure 3, together with selected bond lengths and angles. According to this figure, the position of the atoms Al1 and Al3 is split. The Me groups of the *t*Bu groups at Si2 were refined in the split positions with occupancy factors of 0.5; Al1 and Al2 also have occupancy factors of 0.50. Evidently, the three Al atoms occupy the corners of a triangle with two longer sides (average Al–Al distance: 2.756 Å) and a slightly shorter base (Al–Al distance: 2.703 Å). The atom Al2 at the top of the triangle binds two supersilyl groups and each Al atom of the base is connected

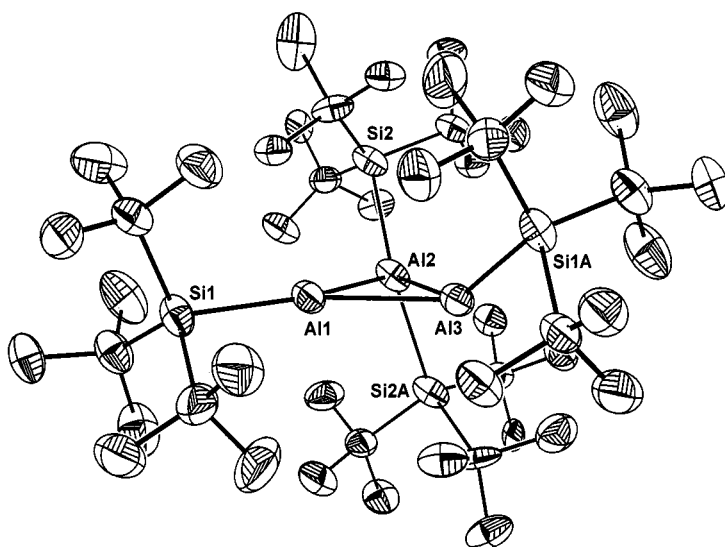


Figure 3. Structure of radicals $R^*_4Al_3\bullet$ (**3**) in the crystal and atom numbering used (ORTEP-Plot; 25% thermal probability ellipsoids; H atoms omitted for clarity); selected distances [Å] and angles [°] in the structure of radical **3** with standard deviations (the positions of Al1 and Al2 are doubly split): Al1–Al2 2.737(2), Al1–Al3 2.703(3), Al2–Al3 2.776(2), Al1–Si1 2.519(1), Al2–Si2 2.556(1), Al3–Si3A 2.586(2); Al2–Al1–Al3 61.35(6), Al1–Al2–Al3 58.33(8), Al2–Al3–Al1 59.92(7), Si1–Al1–Al2 152.6(1), Si1–Al1–Al3 146.0(1) (angle sum at Al1 359.9), Si1A–Al3–Al2 44.5(1), Si1A–Al3–Al1 123.6(1) (angle sum at Al3 328.0), Si2–Al2–Al1 110.48(6), Si2–Al2–Al3 125.47(6), Si2A–Al2–Al1 107.66(6), Si2A–Al2–Al3 90.71(6), Si2–Al2–Si2A 137.28(8)

to only one supersilyl group. The structural data may be interpreted by assuming that the R^*Al groups are more weakly bonded to R^*_2Al than to each other [cf. the Al–Al distance in $R^*_4Al_2$ (2.751 Å)].^[4] If the R^*_2Al group provides one and each R^*Al group two electrons for the Al_3 framework, there are 5 electrons available for the Al_3 cluster. Possibly, the radical electron acts as a π -electron for the

connection of the two R^*Al groups. Intuitively, one might argue that the observed geometry of **3** looks as if cyclisation of *catena*- $[R^*_2Al-R^*Al-AIR^*]\bullet$ (a derivative of **2** with one R^* exchanged by R^*_2Al) – in the course of which the connection of $R^*Al-AIR^*$ becomes weaker, the connection $R^*_2Al\cdots AIR^*$ becomes stronger – is stopped half way on the reaction coordinate (cf. ab initio calculations).

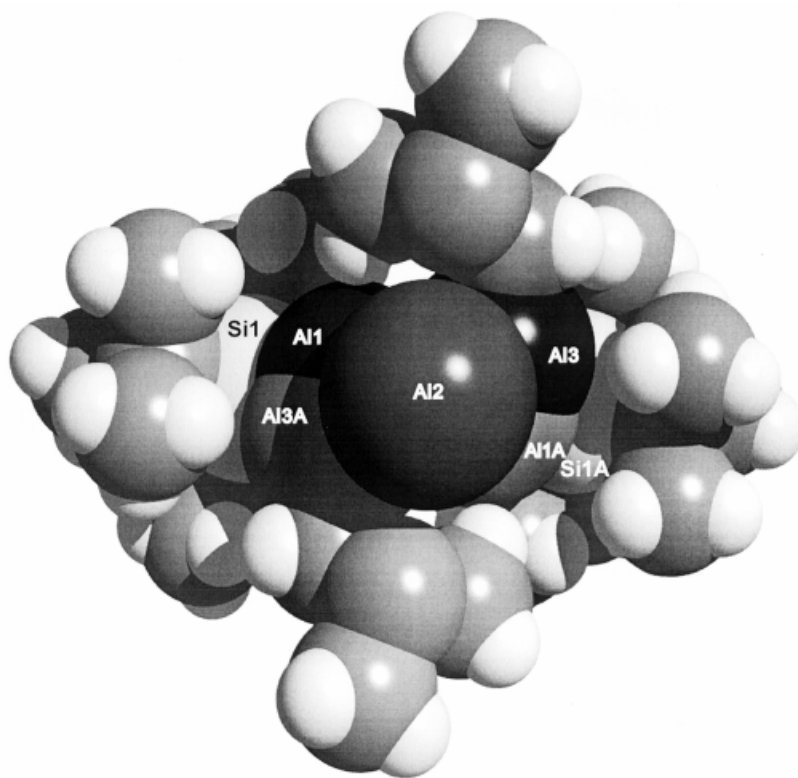


Figure 4. Space filling model of the radical **3** (Si2 and Si2A each with two *t*Bu groups are omitted for clarity)

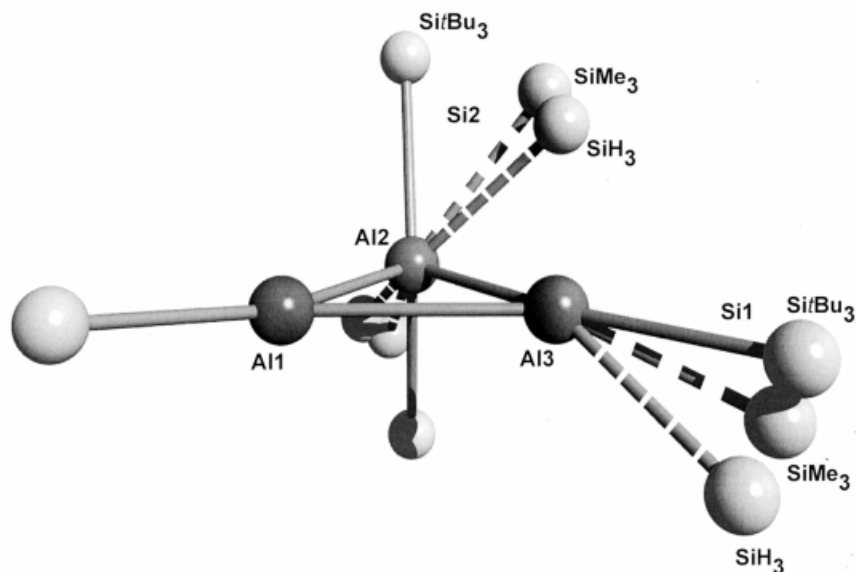


Figure 5. Structure of $R^*_4Al_3^{\bullet}$ with $R = SiH_3, SiMe_3, Si^tBu_3$ as derived from RI-DFT calculations; selected calculated bond lengths [Å] and angles [°] in each case for $(H_3Si)_4Al_3^{\bullet}/(Me_3Si)_4Al_3^{\bullet}/(tBu_3Si)_4Al_3^{\bullet}$: Al1–Al3 2.532/2.645/2.902, Al1–Al2 2.489/2.463/ 2.625, Al2–Al3 3.065/2.560/2.623, Si1–Al3 2.798/2.908/4.292; angle sum at Al1 356.80/ 349.50/360.00, angle sum at Al3 334.43/359.75/360.00

According to Figure 3, the four Si atoms of the supersilyl groups of **3** occupy the corners of a tetrahedron with five edges of roughly equal length (average Si–Si distance: 6.321 Å) and one shorter side which is connected to the atom Al2 in its center (Si–Si distance: 4.760 Å). The reason for the nearly regular tetrahedral packing of the supersilyl groups comes probably from considerable van der Waals attraction between the methyl groups of the substituents R^* .^[13]

The Al atoms of the Al_3 ring now fill up the interstices of the $(R^*)_4$ entity, whereby an arrangement of two planar three-coordinated atoms Al1 and Al3 and, at the same time, of a tetrahedral four-coordinated atom Al3 is obviously impossible. Consequently, in order to fill cavities in the $(R^*)_4$ entity (cf. Figure 4), one of the three-coordinated Al atoms is planar, the other one is pyramidal and the planar Si_2Al is not orthogonal to the plane of Al_3 (cf. Figure 3). Over and above that, the splitting positions of the two atoms Al1 and Al3 point to a fast structural fluctuation of the conformations of the mentioned atoms.

An ab initio calculation (RI-DFT) of the structure of radical **3** differs from the experimentally observed one in several points (cf. Figure 5); in particular, Al2 is tetrahedrally coordinated whereas Al1 and Al3 are each planar coordinated. In addition, the calculated Al1–Al3 distance is much longer than the other Al–Al bonds, contrary to the bonding situation in the experimentally observed structure of **3** (on the other hand, $R^*_4Ga_3^{\bullet}$ shows the predicted structure). Whether this predicted open chain structure is the global minimum was not checked, although it resulted during minimization of the energy, starting from the experimental structure. The structure of radicals $R_4Al_3^{\bullet}$ proved to be dependent on the bulkiness of the four substituents. Therefore, a decrease of bulkiness of the four substituents leads, according to ab initio calculations, to a bonding relation of an Al2 bonded silyl group to Al1 or Al3 (cf. Figure 5), that is a bridging position of a silyl group.

In the ESR spectrum of very dilute solutions of **1** in C_6D_{12} at 80 °C, the typical hyperfine structure of the signal for the radical **2** is observed (Figure 2a). After a few minutes this spectrum disappears. Solutions which are thermolyzed in C_6D_{12} at 80 °C for longer periods of time exhibit a low resolution ESR spectrum: many lines separated by about 1.1 mT are now seen. Obviously, two ESR signals from two different radicals overlap. After leaving this solution for a long time at room temperature, radical **2** reappears in the ESR spectrum. Finally, an ESR spectrum of a dilute solution of pure, isolated radical **3** is shown in Figure 6 (the fact that no NMR signal is detected from this solution confirms the radical character of **3**).

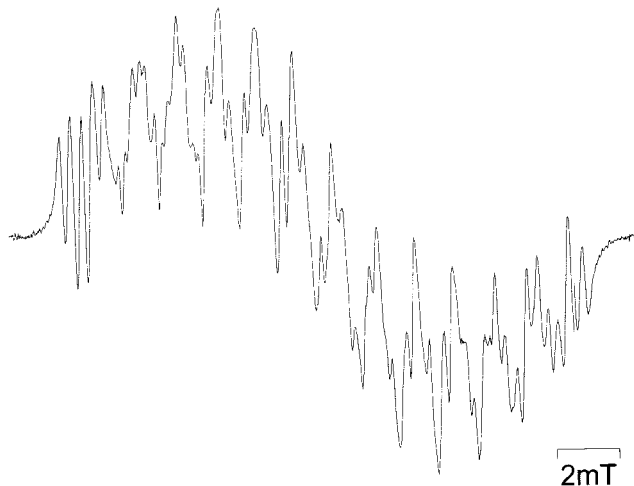


Figure 6. ESR spectrum of **3** in *n*-pentane

The resolution of the ESR spectrum of **3** at room temperature is lower and the number of lines is higher than for the ESR spectrum of **2**. Therefore, the hyperfine structure of the signal, centered at $g = 2.0053$, could not yet be analyzed completely. Besides a clearly determined small coupling

constant for one Al atom of nearly 0.3 mT, two larger and obviously different coupling constants for the second and third Al atoms of nearly 1.3 mT are determined. This assignment is in agreement with the total spectral width of 15.0 mT. According to the g factor and the hyperfine structure, the radical **3** is predominantly a π radical. The smaller ^{27}Al coupling constant may be associated with the four-coordinate Al center (cf. AlR_n -coordinated organic π radicals).^[14,15] On the other hand, the non-equivalence of the two remaining Al centers with hyperfine coupling constants in conventional ranges is well in agreement with the results of the X-ray structure analysis of **3** (see above) and also with an equilibrium $\text{cyclo-3} \rightleftharpoons \text{catena-3}$, where by $\text{R}^*_4\text{Al}_3^\bullet$ shows a cyclic structure in the solid state and a chain structure in solution.

Experimental Section

All experiments were carried out in flame-dried glass apparatus with standard Schlenk techniques under an atmosphere of dry argon or nitrogen. During all manipulations air and moisture were strictly excluded. The solvents (cyclohexane, heptane, pentane, benzene) were distilled from sodium/lead or sodium/benzophenone. For NMR spectra a JEOL GSX-270 ($^1\text{H}/^{13}\text{C}/^{29}\text{Si}$: 270.17/67.94/53.67 MHz) and a JEOL EX-400 ($^1\text{H}/^{13}\text{C}/^{29}\text{Si}$: 399.78/10.54/79.43 MHz) were available. The ^{29}Si NMR spectra were recorded with the INEPT pulse sequence using empirically optimized parameters for polarization transfer from the $t\text{Bu}$ substituents. The ESR spectra were recorded with a Bruker System ESP 300.

Formation of Tri(supersilyl)dialanyl 2: In an evacuated and sealed NMR tube a solution of **1**^[4] (0.020 g, 0.023 mmol) in C_6D_{12} (0.6 mL) was heated to 70 °C for 4 hours and then cooled to room temperature. After this procedure, the black-green solution was found to be free of starting material **1** (by NMR spectroscopy); however, it contained superdisilane $t\text{Bu}_3\text{Si-Si}t\text{Bu}_3$ (identification by comparison with an authentic sample)^[13] and also, according to an ESR spectrum, the radical **2** (not visible in the NMR spectrum). It did not prove possible to isolate crystals of **2** suitable for an X-ray structure analysis.

Formation of Tetra(supersilyl)cyclotriallanyl 3: A solution of **1**^[4] (0.264 g, 0.308 mmol) in heptane (25 mL) was heated to 100 °C for 10 hours (reflux) and then cooled to room temperature. After this procedure, the black-green solution was found to be free of starting material **1** (by NMR spectroscopy); however, it contained supersilane $t\text{Bu}_3\text{Si-H}$, superdisilane $t\text{Bu}_3\text{Si-Si}t\text{Bu}_3$ and **4** [identification by comparison with an authentic samples;^[6,13] $\delta(^1\text{H}; \text{C}_6\text{D}_{12}) = 1.148, 1.382, 1.263$] and also, according to an ESR spectrum, the radical **3** (cf. Figure 6; not visible in the NMR spectrum). The area ratio of the ^1H NMR signals for $t\text{Bu}_3\text{Si-H}$, $t\text{Bu}_3\text{Si-Si}t\text{Bu}_3$ and $(t\text{Bu}_3\text{Si})_4\text{Al}_4$ (**4**) amounts to 6:5:4 (measured for $\text{Si}t\text{Bu}_3$). Consequently, besides one molecule of **4** with four silicon-bonded supersilyl groups, eleven supersilyl radicals are formed which stabilize by formation of $t\text{Bu}_3\text{Si-H}$ and $t\text{Bu}_3\text{Si-Si}t\text{Bu}_3$. Since four $t\text{Bu}_3\text{Si}$ radicals arise during the formation of one molecule of **4** from two molecules of **1** ($2 \times \mathbf{1} \rightarrow \mathbf{4} + 4 t\text{Bu}_3\text{Si}$), $11 - 4 = 7 t\text{Bu}_3\text{Si}$ radicals must come from the formation of **3**. As two $t\text{Bu}_3\text{Si}$ radicals are produced per radical of **3** from 1.5 molecules of **1** ($1.5 \times \mathbf{1} \rightarrow \mathbf{3} + 2 t\text{Bu}_3\text{Si}$), 7 $t\text{Bu}_3\text{Si}$ radicals originate from the formation of 3.5 radicals of **3**. For the formation of 3.5 molecules of **3** and 1 molecule of **4**, therefore, $(3.5 \times 1.5) + (1 \times 2) = 7.25$ molecules of **1**

are needed. Consequently, **3** and **4** are formed in yields of 70 and 30%. In another experiment dialane (0.339 g, 0.395 mmol) was heated in 25 mL cyclohexane at 80 °C for 15 hours. The solvent and all volatile components (C_6H_{12} , $t\text{Bu}_3\text{Si-H}$) were then removed in vacuo and the remaining residue was dissolved in 10 mL heptane. After 2 months tetra(supersilyl)cyclotriallanyl **3** (0.22 g) crystallized from this solution at -25 °C as black-green cubes.

DFT Calculations: All RI-DFT calculations (AL2 and AL3) were carried out with the program package TURBOMOLE with the BP86-Functional and SV(P) basis sets.^[10]

X-ray Structure Determination of 3: Stoe IPDS diffractometer, Mo-K_α radiation with $\lambda = 0.71073 \text{ \AA}$, graphite monochromator, image plate detector, crystal dimensions $0.15 \times 0.20 \times 0.28 \text{ mm}$, fixed on glass fiber, measurement temperature 200(2) K, $\text{C}_{48}\text{H}_{108}\text{Al}_3\text{Si}_4 \cdot 0.25\text{C}_6\text{H}_{14}$, $M_r = 921.73$, black-green rhombus, monoclinic space group $C2/c$, $a = 21.344(4)$, $b = 12.794(3)$, $c = 23.955(5) \text{ \AA}$, $V = 6514(2) \text{ \AA}^3$, $Z = 4$, $\rho_{\text{ber}} = 0.940 \text{ g}\cdot\text{cm}^{-3}$, $\mu = 0.159 \text{ mm}^{-1}$, $F(000) = 2064$. – *Data collection:* $2\theta = 4.08 - 51.84^\circ$ in $-26 \leq h \leq 26$, $-15 \leq k \leq 15$, $-29 \leq l \leq 29$; of 22750 reflections 6316 were independent ($R_{\text{int}} = 0.068$) and 4446 were observed [$F > 4\sigma(F)$], 377 parameters, $R_1 = 0.0887$, $wR_2 = 0.2870$, weighting factor $w^{-1} = \sigma^2 F_o^2 + 0.194P^2$ with $P = F_o^2 + 2F_c/3$. – *Structure determination:* The structure was solved by direct methods (SHELX-97). All non-hydrogen atoms were refined anisotropically, and H atoms were included in the refinement at calculated positions with a riding model and fixed isotropic U_i values. In a distorted arrangement of four supersilyl groups the Al_3 ring is disordered embedded over the C_2 axis. In both positions of the atoms Al1 and Al2 click into free inlets of the $\text{Si}t\text{Bu}_3$ envelope.

Crystallographic data (excluding structure factors) for the structure reported in this paper have been deposited with the Cambridge Crystallographic Data Centre as supplementary publication no CCDC-120209. Copies of this data can be obtained free of charge on application to the Director, CCDC, 12 Union Road, Cambridge CB2 1EZ [Fax: (internat.) + 44-1223/336-033; E-mail: deposit@ccdc.cam.ac.uk].

Acknowledgments

We are grateful to the Deutsche Forschungsgemeinschaft and the Fonds der Chemische Industrie for their generous financial support. We thank Dr. A. Purath for mounting a crystal of the cyclotriallanyl.

[1] Holleman-Wiberg, *Lehrbuch der Anorganischen Chemie*, 101. Auflage, DeGruyter, Berlin, 1995.

[2] W. Uhl, *Angew. Chem.* **1993**, 105, 1449; *Angew. Chem. Int. Ed. Engl.* **1993**, 32, 1386 and references cited therein.

[3] N. Wiberg, K. Amelunxen, H. Nöth, M. Schmidt, H. Schwenk, *Angew. Chem.* **1996**, 108, 110; *Angew. Chem. Int. Ed. Engl.* **1996**, 35, 65 and refs. cited herein.

[4] N. Wiberg, K. Amelunxen, T. Blank, H. Nöth, J. Knizek, *Organometallics* **1998**, 17, 5431 and references cited therein.

[5] N. Wiberg, K. Amelunxen, H.-W. Lerner, H. Nöth, J. Knizek, I. Krossing, *Z. Naturforsch. B*, **1998**, 53, 333.

[6] A. Purath, C. Dohmeier, A. Ecker, H. Schnöckel, K. Amelunxen, T. Passler, N. Wiberg, *Organometallics* **1998**, 17, 1894.

[7] N. Wiberg, K. Amelunxen, H. Nöth, H. Schwenk, W. Kaim, A. Klein, T. Scheiring, *Angew. Chem.* **1997**, 109, 1258; *Angew. Chem. Int. Ed. Engl.* **1997**, 36, 1213 and references cited therein.

[8] N. Wiberg, K. Amelunxen, H.-W. Lerner, H. Nöth, W.

- Ponikwar, H. Schwenk, *J. Organomet. Chem.* **1999**, 574, 246.
- [9] N. Wiberg, T. Blank, H. Nöth, W. Ponikwar, *Angew. Chem.* **1999**, 113, 887; *Angew. Chem. Int. Ed.* **1999**, 38, 839.
- [10] Turbomole: O. Treutler, R. Ahlrichs, *J. Chem. Phys.* **1995**, 102, 346. — Functional BP86: A. D. Becke, *Phys. Rev. A*, **1998**, 38, 3098. — RI DFT: J. P. Peider, *Phys. Rev. B* **1996**, 33, 8822; K. Eichkorn, O. T. Treutler, H. Ohm, M. Häser, R. Ahlrichs, *Chem. Phys. Lett.* **1995**, 242, 612; K. Eichkorn, F. Weigend, O. Treutler, R. Ahlrichs, *Theor. Chem. Acc.* **1997**, 97, 119.
- [11] W. Uhl, U. Schütz, W. Kaim, E. Waldhör, *J. Organomet. Chem.* **1995**, 501, 79.
- [12] W. Uhl, A. Vester, W. Kaim, J. Poppe, *J. Organomet. Chem.* **1993**, 454, 9.
- [13] N. Wiberg, *Coord. Chem. Rev.* **1997**, 163, 217.
- [14] W. Kaim, *Z. Naturforsch. B* **1981**, 36, 677.
- [15] W. Kaim, *J. Organomet. Chem.* **1981**, 215, 325.

Received December 27, 1999
[199474]